Assessing the Roles of the Constituents of Ionic Liquids in Dynamic Solvation: Comparison of an Ionic Liquid in Micellar and Bulk Form

Prasun Mukherjee,[†] Jeffrey A. Crank,[‡] Mintu Halder,[†] Daniel W. Armstrong,[‡] and Jacob W. Petrich*,[†]

Department of Chemistry, Iowa State University, Ames, Iowa 50011, and Department of Chemistry and Biochemistry, University of Texas, Arlington, Box 19065, Arlington, Texas 76019

Received: June 2, 2006; In Final Form: July 21, 2006

Dynamic solvation of the dye, coumarin 153, is compared in an ionic liquid that forms micelles in water against the bulk solvent. This provides the unprecedented opportunity of investigating the behavior of the ionic liquid in two globally different configurations. It is proposed that the imidazolium moiety is in both cases responsible for the majority of the solvation, which manifests itself in the first 100 ps. Exploiting the use of ionic liquids capable of accommodating specific structures thus provides a deeper insight into how solutes interact with these fascinating and interesting solvents (at least those that are imidazolium based) that are gaining ever increasing interest in the scientific community.

Introduction

Room temperature ionic liquids, most commonly comprised of organic cations and inorganic anions, are receiving an increasing amount of attention because of their utility as environmentally friendly, "green" solvents and because of a host of practical applications to which they are amenable.[1−4] The importance of ionic liquids has consequently stimulated considerable interest in their dynamic solvation properties, both in the experimental[5−25] and the theoretical arenas.[26−32] An intriguing aspect of certain ionic liquids, which has only recently become appreciated, is their ability to promote micelle formation or to form micelles themselves.[33−36] Major questions regarding dynamic solvation by ionic liquids deal with whether the organic cation or the inorganic anion solvate preferentially on different time scales, the role of the correlated motion of the ion pairs and their lifetime, and the importance of translational motion of the ions relative to dipolar relaxation.[23−25] Here, we attempt to address some of these questions by studying the solvation of the dye, coumarin 153, in a bulk ionic liquid and its corresponding micelle in water (Figure 1). Because coumarin 153 is only sparingly soluble and weakly fluorescent in water, a clear distinction can be made between its fluorescent properties in the bulk ionic liquid and that in the micelles formed from the ionic liquid. Sarkar and co-workers[37] have compared the solvation dynamics of coumarin 153 in an ionic liquid with that of coumarin 153 in Brij-35 micelles in the same ionic liquid. This comparison suffers because coumarin 153 is soluble in both systems and only modest differences can be observed. Hara et al. have performed a detailed study of the effect of pressure on the solvation of coumarin 153 in micelles.[38]

Materials and Methods

Ionic Liquid Synthesis. 1-Cetyl-3-vinylimidazolium bromide was synthesized by reacting 1 molar equivalent of 1-vinylimidazole and 1-bromohexadecane. The mixture was heated to 65 °C and stirred for 4 h. The bromide salt was then dissolved in water and heated to 50 °C for hot extraction. Eight extractions were performed with ethyl acetate to remove impurities. The ionic liquid was then allowed to crystallize in the aqueous solution to purify the product further. The ionic liquid was then filtered and dried under vacuum. Anion exchange of 1-cetyl-3-vinylimidazolium bromide to 1-cetyl-3-vinylimidazolium bis-[(trifluoromethyl)sulfonyl]imide (NTf$_2$) was achieved by first dissolving the bromide salt in water. Next an equimolar amount of lithium bis[(trifluoromethyl)sulfonyl]imide was dissolved in water and added to the bromide salt solution and stirred until the aqueous layer became clear. The NTf$_2$ salt was then dissolved in methylene chloride and extracted with water eight times. A rotary evaporator was used to remove the excess methylene chloride. The NTf$_2$ salt was then placed under vacuum overnight to achieve complete dryness. Viscosity measurements for the solvents studied were taken with a ViscoLab 4000 piston-style viscometer from Cambridge Applied Systems.

CMC Determination. The critical micelle concentration (CMC) was found by plotting surface tension (dyn/cm) against concentration (mM). Surface tension measurements were taken using a Fischer Model 20 surface tensiometer. All glassware used was cleaned by chromic acid, rinsed with deionized water, and dried in an oven. Concentrations between 0 and 1×10^{-3} M of 1-cetyl-3-vinylimidazolium bromide were prepared in aqueous solution and heated to 39 °C. Measurements were taken at 39 °C to circumvent solubility problems that occur at room temperature. An average of four measurements was taken to obtain the surface tension at each concentration of the ionic liquid. At 21 °C, CMC = 2.6×10^{-5} M; at 39 °C, CMC = 3.2×10^{-5} M.

Determination of the Micellar Aggregation Number. The aggregation number (the average number of surfactant molecules per micelle) can be estimated by optical techniques proposed by Turro and Yekta[39] and later modified by De Schryver and co-workers.[40] We employ the latter method, where the micellar aggregation number is obtained by exploiting the vibronic fine structure of pyrene emission. Pyrene was recrystallized several

* To whom correspondence should be addressed.
† Iowa State University.
‡ University of Texas, Arlington.
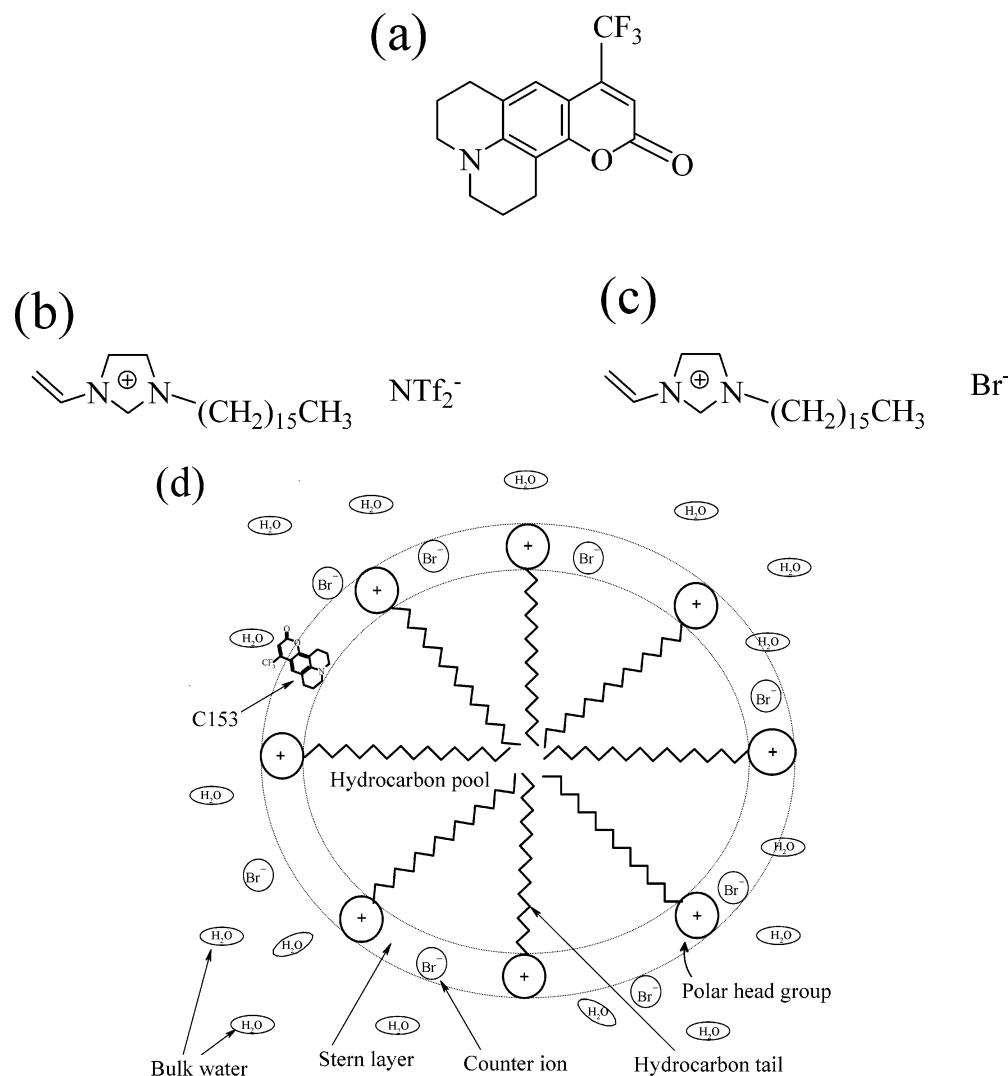
Figure 1. Structures of the (a) solvation probe, coumarin 153 (C153), and the two ionic liquids, (b) 1-cetyl-3-vinylimidazolium NTf₂ ([CVIM⁺][NTf₂⁻], NTf₂⁻ = (CF₃SO₂)₂N⁻; melting point, 39 °C), and (c) 1-cetyl-3-vinylimidazolium bromide ([CVIM⁺][Br⁻]; melting point, 69 °C). The bromide salt forms micelles in water. Also provided is a schematic diagram (d) of the micelle formed by [CVIM⁺][Br⁻], in water indicating the proposed location of C153 in the Stern layer.

times from absolute ethanol before use. Three stock solutions were prepared of concentrations 0.2×10^{-3}, 10×10^{-3}, and 4×10^{-2} M pyrene in ethanol, cetyl pyridinium chloride in water, and [CVIM⁺][Br⁻] in water, respectively. For all measurements, pyrene and surfactant concentrations were kept constant at ~2×10^{-6} M and ~4×10^{-3} M. Six solutions were prepared with increasing quencher concentration from 0 to 0.5×10^{-3} M. Samples were excited at 337 nm for emission spectra. The aggregation number can be determined using eqs 1 and 2

$$\ln\left(\frac{I_0}{I_Q}\right) = \frac{[Q_{mic}]}{[mic]} \qquad (1)$$

where I_0 is the emission intensity at a particular wavelength in the absence of added quencher and I_Q is the corresponding emission intensity in the presence of quencher and micelle concentrations of $[Q_{mic}]$ and $[mic]$, respectively. The mean aggregation number, $\langle a \rangle$, is given by

$$\langle a \rangle = \frac{[S_{tot}] - CMC}{[mic]} \qquad (2)$$

Cetyl pyridinium chloride can also form micelles, so in the present case the $[Q_{mic}]$ is not exactly equal to the total quencher

concentration, $[Q_{tot}]$. The $[Q_{mic}]$ were calculated using

$$[Q_{mic}] = (1 - \alpha)[Q_{tot}] \qquad (3)$$

where

$$\alpha = \frac{CMC}{[S_{tot}]} \qquad (4)$$

A plot of $\ln(I_0/I_Q)$ against $[Q_{mic}]$ yields a straight line with a slope of $1/[mic]$ (eq 1). Multiplying the slope with the difference between the total surfactant concentration and the critical micellar concentration (CMC) gives the mean aggregation number (eq 2). Calculations can be performed using the intensity of either band I or band III. We have chosen the emission intensity of band I (at ~373 nm) or band III (at ~384 nm) for determining the aggregation number of the micelle. The results obtained from both bands were identical. The mean aggregation number of [CVIM⁺][Br⁻] micelle at 39 °C was found to be 25.

Preparation of Micellar Solutions. The CMC of [CVIM⁺][Br⁻] in water was found to be 3.2×10^{-5} M at 39 °C; see above. For all experiments in micellar systems, the C153 concentration was kept at ~8×10^{-6} M in ~4×10^{-3} M [CVIM⁺][Br⁻] (~125 times CMC) and a 500:1 surfactant-to-

Constituents of Ionic Liquids in Dynamic Solvation

J. Phys. Chem. A, Vol. 110, No. 37, 2006 **10727**

C153 ratio was maintained. Under these conditions there is one C153 molecule for every 20 micelles, thus minimizing the possibility of association or contact between the C153 probes.

Preparation of Solutions for Stern–Volmer Quenching Experiments. For quenching of C153 in methanol, two stock solutions were prepared of concentrations 2×10^{-4} M C153 in methanol and 0.5 M potassium iodide in methanol. For all measurements, C153 concentrations were kept constant at $\sim 2 \times 10^{-6}$ M. Six solutions were prepared with increasing quencher concentration from 0 to 0.4 M. Similar quenching experiments were performed in micellar environment by preparing three stock solutions of concentrations 2×10^{-4}, 4×10^{-2}, and 0.1 M, of C153 in methanol, [CVIM$^+$][Br$^-$] in water, and potassium iodide in water, respectively. For all measurements, C153 and surfactant concentrations were kept constant at $\sim 2 \times 10^{-6}$ and $\sim 4 \times 10^{-3}$ M. Six solutions were prepared with increasing quencher concentration from 0 to 2×10^{-2} M. Samples were excited at 420 nm for taking the emission spectra.

Steady-State Optical Measurements. Steady-state excitation and emission spectra were recorded with a SPEX Fluoromax with a 4-nm band-pass and were corrected for detector response. A 1-cm path length quartz cuvette was used for the measurements except for [CVIM$^+$][Br$^-$] as a pure solvent. For this system, a 5-mm path length quartz cuvette was used. During spectroscopic measurements, the quartz cuvettes were kept tightly sealed so as to prevent moisture from being absorbed by the ionic liquids. The steady-state spectra can be used to compute the reorganization energy, λ[23,24]

$$\lambda = \hbar \frac{\int_0^\infty d\nu [\sigma_a(\nu) - \sigma_f(\nu)]\nu}{\int_0^\infty d\nu [\sigma_a(\nu) + \sigma_f(\nu)]} \quad (5)$$

The $\sigma_{a,f}$ are the absorption (or excitation) and emission spectral line-shapes, respectively.

Time-Resolved Measurements. The apparatus for the time-correlated single-photon counting measurements is described in detail elsewhere.[23,24] The instrument response function had a full width at half-maximum (fwhm) of ≤ 100 ps. A 1-cm path length quartz cuvette was used for all the time-resolved measurements except for [CVIM$^+$][Br$^-$] as pure solvent. A 5-mm path length quartz cuvette was used for this solvent. To construct the time-resolved spectra, a series of decays (~ 3000 counts in the peak channel) were collected over as much of the fluorescence spectrum as possible, typically from 470 to 610 nm at 10 nm intervals. They were fit to a maximum of three exponentials. Transient spectra were reconstructed from these fits by normalizing to the steady-state spectra:

$$S(\lambda,t) = D(\lambda,t) \frac{S_0(\lambda)}{\int_0^\infty D(\lambda,t)} \quad (6)$$

$D(\lambda,t)$ is the wavelength-resolved fluorescence decay, and $S_0(\lambda)$ is the steady-state emission intensity at a given wavelength. We have employed the traditional approach of fitting the time-resolved spectra to a log-normal function, from which we extract the peak frequency, $\nu(t)$, as a function of time.

The solvation dynamics were described by the normalized correlation function:

$$C(t) = \frac{\nu(t) - \nu(\infty)}{\nu(t=0) - \nu(\infty)} \quad (7)$$

$\nu("t=0")$ is the frequency at zero time.[24,41] $\nu(\infty)$ is the frequency
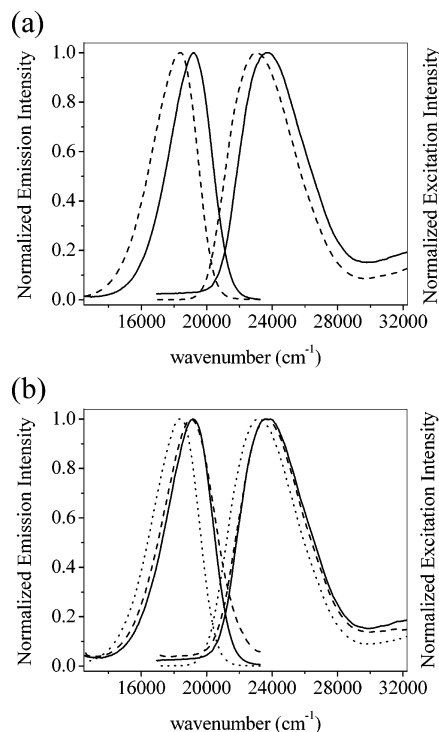
Figure 2. (a) Normalized excitation and emission spectra of C153 in [CVIM$^+$][NTf$_2^-$] (solid line) and in [CVIM$^+$][Br$^-$] under micellar conditions (dashed line) at 39 °C; (b) normalized excitation and emission spectra of coumarin 153 in [CVIM$^+$][NTf$_2^-$] (solid line), in [CVIM$^+$][Br$^-$] (dashed line), and in [CVIM$^+$][Br$^-$] under micellar conditions (dotted line) at 69 °C.

at "infinite time," the maximum of the steady-state fluorescence spectrum. $\nu(t)$ is determined by taking the maxima from the log-normal fits as the emission maximum. In most of the cases, however, the spectra are broad, so there is some uncertainty in the exact position of the emission maxima. Thus, we have considered the range of the raw data points in the neighborhood of the maximum to estimate an error for the maximum obtained from the log-normal fit. Depending on the width of the spectrum (i.e. "zero-time", steady-state, or time-resolved emission spectrum), we have determined the typical uncertainties as follows: zero-time $\sim$ steady-state ($\sim \pm 100$ cm^{-1}) $<$ time-resolved emission ($\sim \pm 200$ cm^{-1}). We use these uncertainties to compute error bars for the $C(t)$.

Finally, in generating the $C(t)$, the first point was obtained from the zero-time spectrum. The second point was taken at the maximum of the instrument response function, which, having a fwhm ≤ 100 ps, was taken to be ~ 100 ps. Fractional solvation at 100 ps was calculated using $f(t=100\text{ps}) = 1 - C(t=100\text{ps})$.

Polarized fluorescence traces were collected in order to obtain anisotropy decay parameters. 10 000 counts were collected in the peak channel of the trace whose polarization was aligned parallel to that of the excitation pulse. We could not detect any polarized fluorescence from coumarin 153 dissolved in [CVIM$^+$][Br$^-$] (solvent). This might be due to scattering arising from the opaque, solid substance formed at 69 °C.

Results

Steady-state spectra and representative wavelength-resolved decays are presented in Figures 2 and 3, respectively. Figure 4 provides the solvation relaxation functions, $C(t)$. Relevant spectroscopic and relaxation parameters are summarized in Tables 1 and 2. Examination of Figure 4 and Table 1 indicates the following.
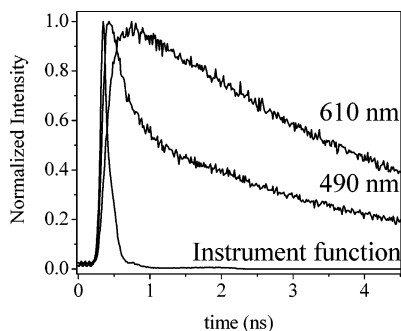
Figure 3. Representative wavelength-resolved decays for C153 at 490 and 610 nm in [CVIM$^+$][Br$^-$] under micellar conditions at 39 °C. A typical instrument response function is shown. The decay at blue end of the spectrum decays faster than that of at the red end of the spectrum. The decay at the red end of the spectrum shows a growing component. The decays used to construct the time-resolved emission spectra were typically collected over a range of wavelengths from 470 to 610 nm at 10 nm intervals; a total of 15 decays were used to generate the time-resolved emission spectra, from which the $C(t)$ values were calculated.
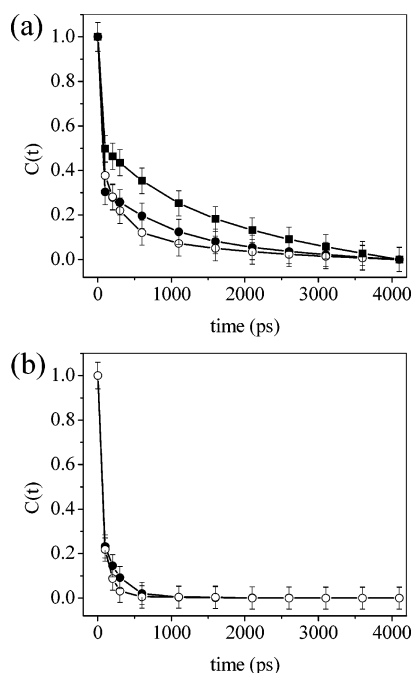
Figure 4. $C(t)$ curves for C153: (a) [CVIM$^+$][NTf$_2^-$] (bulk solvent) at 39 °C (solid circles), [CVIM$^+$][NTf$_2^-$] (bulk solvent) at 69 °C (open circles), and [CVIM$^+$][Br$^-$] (bulk solvent) at 69 °C (squares); (b) [CVIM$^+$][Br$^-$] (micelle) at 39 °C (solid circles) and [CVIM$^+$][Br$^-$] (micelle) at 69 °C (open circles). In all cases, the initial fast component of solvation occurs within our instrumental time resolution. See Table 1.

1. Temperature does not significantly (within 10%) change the fractional solvation at 100 ps or the average solvation time for either bulk [CVIM$^+$][NTf$_2^-$] or for micellar [CVIM$^+$][Br$^-$].

2. The fractional solvation of bulk [CVIM$^+$][NTf$_2^-$] and micellar [CVIM$^+$][Br$^-$] are comparable: 0.70, 0.62; 0.77, 0.78, respectively. There is roughly 10% more unresolved solvation occurring in the micelle. It is unclear how much of this additional solvation occurs because of the difference in the anion or because of the difference between the bulk or micellar systems. To respond to this question, it is crucial to study bulk [CVIM$^+$][Br$^-$].

3. It is to be noted that, of the systems considered here, only [CVIM$^+$][Br$^-$] forms micelles in water and that bulk [CVIM$^+$][Br$^-$] forms an opaque solid that is suitable for measurements of spectra and lifetimes, but scatters light to such

a degree that it is not suitable for obtaining measurements of polarized fluorescence. Nonetheless, it is striking that in the solid bulk, [CVIM$^+$][Br$^-$] still has f_{100ps} as great as 0.50. For example, Maroncelli and co-workers, using an instrument response of 25 ps, found that, for the imidazolium ionic liquid, [DMPIM$^+$][NTf$_2^-$], whose glass transition temperature is ~191 K, 0.54 of the solvation is missed at 323 K, whereas only 0.17 is missed at 238 K.[11]

4. The fluorescence anisotropies (Table 2) computed from the polarized fluorescence data indicate a single-exponential decay for bulk [CVIM$^+$][NTf$_2^-$]. On the other hand, for micellar [CVIM$^+$][Br$^-$], the anisotropy decay is dominated by a sub-picosecond component and accompanied by a very long component whose duration could not be determined on the time scale employed for the measurement. The former is attributed to rapid restricted movement of the coumarin 153; and the slower, to overall tumbling of the micelle.

5. Stern–Volmer quenching data indicate that coumarin 153 is quenched more easily when it is embedded in micellar [CVIM$^+$][Br$^-$] than in methanol solution (Figure 5).

Discussion

The above results lead us to suggest the following.

1. Coumarin 153 is located in the Stern layer of the [CVIM$^+$][Br$^-$]. This seems reasonable since coumarin 153 is expected to be more soluble in a polarizable environment dominated by imidazolium than a long, nonpolarizable hydrocarbon chain. It is also well-known that coumarin 153 is sparingly soluble and weakly fluorescent in bulk water. More concrete justification of this assignment is given by the anisotropy and the quenching data. The fluorescence anisotropy is dominated by a rapid phase, which is consistent with a mobile coumarin probe located near the micellar surface. This is also confirmed by the quenching data. Coumarin 153 is more strongly quenched in the micelle, whose cationic headgroups exert a Coulombic attraction upon the anionic quencher, I$^-$.

2. The same entity is responsible for the majority of the solvation in both bulk [CVIM$^+$][NTf$_2^-$] and micellar [CVIM$^+$][Br$^-$]. We suggest, as we have elsewhere,[23–25] that it is the imidazolium cation. It has been proposed that the NTf$_2^-$ may play a major role in solvation because of its polarizability and flexibility.[17,24] At least in this example, that does not seem to be the case: f_{100ps} is slightly larger for micellar [CVIM$^+$][Br$^-$] than for bulk [CVIM$^+$][NTf$_2^-$].

3. The slightly enhanced f_{100ps} observed in micellar [CVIM$^+$][Br$^-$] is attributed to water molecules that are localized near the Stern layer. The average solvation time is considerably shorter in micellar [CVIM$^+$][Br$^-$] than in bulk [CVIM$^+$][NTf$_2^-$], about 70 ps as opposed to 300 ps. The former solvation time is nowhere near that of bulk water, where solvation is essentially complete after 1 ps.[42,43] It is known, however, that water in confined environments produces solvation that is significantly slower than that of bulk,[43,44] and thus, the average solvation time observed for micellar [CVIM$^+$][Br$^-$] is consistent with the presence of water molecules that are confined by the Stern layer. It is also possible, however, that the slower solvation in the bulk solvents arises at least in part from the higher viscosity of these systems (Table 1).

Conclusions

As noted above, our previous work on ionic liquids has led us to conclude that the organic cation is most often responsible for the early-time dynamic solvation events.[23–25] Here we compare the micellar system formed by 1-cetyl-3-vinylimida-

Constituents of Ionic Liquids in Dynamic Solvation

J. Phys. Chem. A, Vol. 110, No. 37, 2006 **10729**

TABLE 1: Solvation of Coumarin 153 in Bulk and Micellar Ionic Liquid Systems

system	η (cP)	$\lambda_{t=0}$ (cm^{-1})	λ_{SS} (cm^{-1})	$f_{100\ ps}$	$a_1{}^a$	τ_1 (ps)	τ_2 (ps)	$\langle\tau\rangle$ (ns)
[CVIM$^+$][NTf$_2{}^-$] bulk (39 °C)	124 ± 2.5	1924	2590	0.70	0.67	1	1130	0.37
[CVIM$^+$][NTf$_2{}^-$] bulk (69 °C)	37.5 ± 0.8	1906	2616	0.62	0.44	2	1180	0.28
[CVIM$^+$][Br$^-$] bulk (69 °C)	solid	1985	2716	0.50	0.46	0.3	1420	0.77
[CVIM$^+$][Br$^-$] micelle (39 °C)	0.67 ± 0.01	1854	2720	0.77	0.63	2	220	0.08
[CVIM$^+$][Br$^-$] micelle (69 °C)	0.37 ± 0.01	1898	2748	0.78	0.44	2	110	0.06

^{a} The solvation relaxation functions, $C(t)$, are in all cases but one fit to a sum of two decaying exponentials: $C(t) = a_1 \exp(-t/\tau_1) + a_2 \exp(-t/\tau_2)$, where $a_1 + a_2 = 1$. The exception is [CVIM$^+$][NTf$_2{}^-$] bulk at 69 °C, where there is an intermediate time constant of 190 ps with a weight of 0.38. The average solvation time, $\langle\tau\rangle$, is given by the sum of the products of the preexponential factors and the time constants. Although we fit the $C(t)$ to a sum of exponentials, we do not intend to suggest that this presents an accurate physical description of the solvation process. Finally, we note that the magnitude of τ_1, and consequently that of $\langle\tau\rangle$, is an estimate obtained essentially from only two data points, that at "zero time" and that at 100 ps. Consequently, the very early time process may be considerably more complicated or represented by a much shorter time constant.

TABLE 2: Fluorescence Anisotropy of Coumarin 153 in Bulk Solvents and Micellar Systems

system	$r_0{}^a$	$\tau^{(r)}{}_1$ (ns)	r_1	$\tau^{(r)}{}_2$ (ns)	r_2	$\langle\tau^{(r)}\rangle^a$ (ns)
[CVIM$^+$][NTf$_2{}^-$] bulk(39 °C)	0.32 ± 0.03	3.5	0.32			3.5
[CVIM$^+$][NTf$_2{}^-$] bulk (69 °C)	0.29 ± 0.02	1.6	0.29			1.6
[CVIM$^+$][Br$^-$] micelle (39 °C)	0.24 ± 0.02	0.46	0.23	>20	0.01	
[CVIM$^+$][Br$^-$] micelle (69 °C)	0.22 ± 0.03	0.24	0.18	>20	0.04	

^{a} The errors for r_0 are based on the average of three measurements. The bulk solvents yielded a single-exponential anisotropy decay. The fitting parameters are estimated to be accurate to approximately ±15%. An average anisotropy decay time is not computed for the micellar systems, since the longer decay components could not be accurately determined on the time scale used, 12 ns full scale.
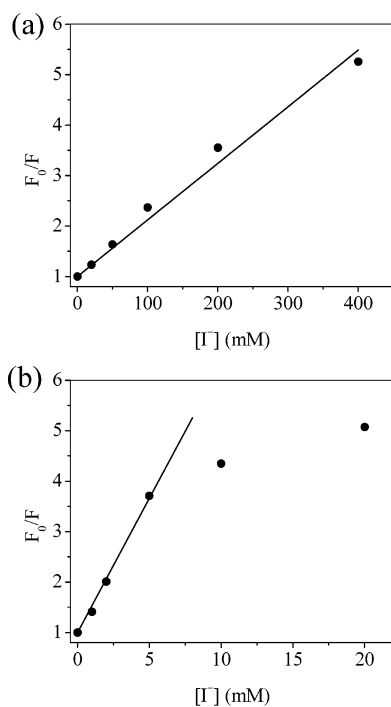
Figure 5. Stern−Volmer quenching plots of C153 in (a) methanol and (b) [CVIM$^+$][Br$^-$] micelle. K_{SV} values were found to be 10 M^{-1} for C153 in methanol and 530 M^{-1} for [CVIM$^+$][Br$^-$] micelle. For the micellar system we have fit only the initial linear portion of the data. The very efficient quenching of C153 fluorescence in micelle is indicative of the presence of probe molecule in the Stern layer of the micelle (see text). All experiments were done at 39 °C.

zolium bromide in water against the bulk bromide solvent and the NTf$_2{}^-$ solvent (Figure 1). Given that coumarin 153 is sparingly soluble in both water and nonpolar hydrocarbons, it is most likely that it is located in the Stern layer of the micelle formed by 1-cetyl-3-vinylimidazolium bromide. If this is so, the immediate environment of the coumarin is predominantly the imidazolium cation and an outer sphere of associated water molecules and bromide ions (Figure 1d). Table 1 and Figure 4 indicate that the fractional solvation in the micelles is, within experimental error, slightly greater than or equal to that in the

bulk ionic liquids. We interpret this result as indicative of predominant solvation in both cases by the imidazolium cation. This assignment, however, is tentative since it is based only upon the value of the fractional solvation at 100 ps. To make it definitive, solvation studies need to be performed either on a variety of ionic liquids and counteranions or with superior time resolution so that the form of the $C(t)$ function may be compared. Finally, the average solvation time in the micelles is considerably smaller than that of the bulk solvents, which we interpret in terms of the contribution of localized water molecules.

Exploiting the use of ionic liquids capable of accommodating specific structures provides a deeper insight into how solutes interact with these fascinating and interesting solvents that are gaining ever increasing interest in the scientific community.

References and Notes

(1) Seddon, K. R. *Nat. Mater.* **2003**, *2*, 363.

(2) Anderson, J. L.; Ding, J.; Welton, T.; Armstrong, D. W. *J. Am. Chem. Soc* **2002**, *124*, 14247.

(3) Anderson, J. L.; Armstrong, D. W.; Wei, G.-T. *Anal. Chem.* **2006**, *78*, 2893.

(4) Pandey, S. *Anal. Chim. Acta* **2006**, *556*, 38.

(5) Karmakar, R.; Samanta, A. *J. Phys. Chem. A* **2002**, *106*, 6670.

(6) Karmakar, R.; Samanta, A. *J. Phys. Chem. A* **2002**, *106*, 4447.

(7) Karmakar, B.; Samanta, A. *J. Phys. Chem. A* **2003**, *107*, 7340.

(8) Ingram, J. A.; Moog, R. S.; Ito, N.; Biswas, R.; Maroncelli, M. *J. Phys. Chem. B* **2003**, *107*, 5926.

(9) Ito, N.; Arzhantsev, S.; Maroncelli, M. *Chem. Phys. Lett.* **2004**, *396*, 83.

(10) Ito, N.; Arzhantsev, S.; Heitz, M.; Maroncelli, M. *J. Phys. Chem. B* **2004**, *108*, 5771.

(11) Arzhantsev, S.; Ito, N.; Heitz, M.; Maroncelli, M. *Chem. Phys. Lett.* **2003**, *381*, 278.

(12) Arzhantsev, S.; Hui, J.; Baker, G. A.; Naoki, I.; Maroncelli, M. Solvation dynamics in ionic liquids, results from ps and fs emission spectroscopy. In *Femtochemistry VII*; Castleman, A. W., Ed.; Elsevier: New York, 2005.

(13) Arzhantsev, S.; Hui, J.; Naoki, I.; Maroncelli, M. *Chem. Phys. Lett.* **2006**, *417*, 524.

(14) Hyun, B.-R.; Dzyuba, S. V.; Bartsch, R. A.; Quitevis, E. L. *J. Phys. Chem. A* **2002**, *106*, 7579.

(15) Giraud, G.; Gordon, C. M.; Dunkin, I. R.; Wynne, K. *J. Chem. Phys.* **2003**, *119*, 464.

(16) Cang, H.; Li, J.; Fayer, M. D. *J. Chem. Phys.* **2003**, *119*, 13017.

(17) Shirota, H.; Funston, A. M.; Wishart, J. F.; Castner, E. W., Jr. *J. Chem. Phys.* **2005**, *122*, 184512/1.

(18) Rajian, J. R.; Li, S.; Bartsch, R. A.; Quitevis, E. L. *Chem. Phys. Lett.* **2004**, *393*, 372.

(19) Shirota, H.; Castner, E. W., Jr. *J. Phys. Chem. A* **2005**, *109*, 9388.

(20) Weingartner, H.; Knocks, A.; Schrader, E.; Kaatze, U. *J. Phys. Chem. A* **2001**, *105*, 8646.

(21) Daguenet, C.; Dyson, P. J.; Krossing, I.; Oleinikova, A.; Slattery, J.; Wakai, C.; Weingartner, H. *J. Phys. Chem. B*, accepted.

(22) Ito, N.; Huang, W.; Richert, R. *J. Phys. Chem. B* **2006**, *110*, 4371.

(23) Chowdhury, P. K.; Halder, M.; Sanders, L.; Calhoun, T.; Anderson, J.; Armstrong, D. W.; Song, X.; Petrich, J. W. *J. Phys. Chem. B* **2004**, *108*, 10245.

(24) Headley, L. S.; Mukherjee, P.; Anderson, J. L.; Ding, R.; Halder, M.; Armstrong, D. W.; Song, X.; Petrich, J. W. *J. Phys. Chem. A* **2006**, *110*, 9549.

(25) Halder, M.; Headley, L. S.; Mukherjee, P.; Song, X.; Petrich, J. W. *J. Chem. Phys. A* **2006**, *110*, 8623.

(26) Margulis, C. J.; Stern, H. A.; Berne, B. J. *J. Phys. Chem. B* **2002**, *106*, 12017.

(27) Shim, Y.; Duan, J.; Choi, M. Y.; Kim, H. J. *J. Chem. Phys.* **2003**, *119*, 6411.

(28) Znamenskiy, V.; Kobrak, M. N. *J. Phys. Chem. B* **2004**, *108*, 1072.

(29) Kobrak, M. N.; Znamenskiy, V. *Chem. Phys. Lett.* **2004**, *395*, 127.

(30) Del Popolo, M. G.; Voth, G. A. *J. Phys. Chem. B* **2004**, *108*, 1744.

(31) Morrow, T. I.; Maginn, E. J. *J. Phys. Chem. B* **2002**, *106*, 12807.

(32) Hu, Z.; Margulis, C. J. *Proc. Natl. Acad. Sci. U.S.A.* **2006**, *103*, 831.

(33) Anderson, J. L.; Pino, V.; Hagberg, E. C.; Sheares, V. V.; Armstrong, D. W. *Chem. Commun. (Cambridge)* **2003**, *19*, 2444.

(34) Trewyn, B. G.; Whitman, C. M.; Lin, V. S. Y. *Nano Lett.* **2004**, *4*, 2139.

(35) Miskolczy, Z.; Sebok-Nagy, K.; Biczok, L.; Gokturk, S. *Chem. Phys. Lett.* **2004**, *400*, 296.

(36) Merrigan, T. L.; Bates, E. D.; Dorman, S. C.; Davis, J. H., Jr. *Chem. Commun.* **2000**, 2051.

(37) Chakraborty, A.; Seth, D.; Chakrabarty, D.; Setua, P.; Sarkar, N. *J. Phys. Chem. A* **2005**, *109*, 11110.

(38) Hara, K.; Baden, N.; Kajimoto, O. *J. Phys.: Condens. Matter* **2004**, *16*, S1207.

(39) Turro, N. J.; Yekta, A. *J. Am. Chem. Soc.* **1978**, *100*, 5951.

(40) Stam, J. v.; Depaemelaere, S.; De Schryver, F. C. *J. Chem. Educ.* **1998**, *75*, 93.

(41) Fee, R. S.; Maroncelli, M. *Chem. Phys.* **1994**, *183*, 235.

(42) Jimenez, R.; Fleming, G. R.; Kumar, P. V.; Maroncelli, M. *Nature* **1994**, *369*, 471.

(43) Vajda, S.; Jimenez, R.; Rosenthal, S. J.; Fidler, V.; Fleming, G. R.; Castner, E. W. *J. Chem. Soc., Faraday Trans.* **1995**, *91*, 867.

(44) Pal, S. K.; Peon, J.; Bagchi, B.; Zewail, A. H. *J. Phys. Chem. B* **2002**, *106*, 12376.